JOURNAL OF MATERIALS SCIENCE 27 (1992) 5623–5628

Internal oxidation of rapidly solidified silver–tin–indium alloy powders

A. VERMA, T.R. ANANTHARAMAN
Thapar Corporate Research and Development Centre, Patiala 147001, India

The internal oxidation behaviour of rapidly solidified silver–tin–indium (Ag–Sn–In) alloy powders is described. Internal oxidation of Ag–Sn–In alloy has gained importance in view of the possible replacement of toxic silver–cadmium oxide (Ag–CdO) material by a better property silver–tin oxide ($Ag–SnO_2$) electrical contact material. Rapidly solidified Ag–Sn–In alloy powders of composition Ag–6.0Sn–3.0In were prepared by gas atomization. The important characteristics of alloy and powders, from the point of view of internal oxidation, were determined. The powders were internally oxidized and subsequently processed by conventional powder metallurgy techniques. The important physical properties, such as electrical conductivity, hardness, density and microstructure, were determined. The physical properties, especially the microstructure and rate of internal oxidation, were compared with the materials prepared by the conventional internal oxidation route.

1. Introduction

Various facets of internal oxidation of silver-based binary alloys have been studied by many researchers [1–3]. The process basically involves diffusion of oxygen through an alloy consisting of a noble and one or more less noble component(s). Formation of oxides of less noble component(s) takes place *in situ*, if its free energy of oxide formation is lower than that of the noble metal. The kinetics of the process for a binary system has been worked out by Rhines *et al.* [4]. The results of these studies have been used to develop various silver–metal oxide electrical contact materials, such as silver–cadmium oxide, silver–tin oxide, silver–indium oxide, etc. However, internal oxidation of materials is intrinsically slow and results in a non-uniform dispersion of oxides as well as an oxide-free zone, also called a denuded zone, in the centre.

In order to overcome some of these problems with varying degree of success, internal oxidation of alloyed powder (IOAP) of various silver-based alloys has been tried [5]. IOAP not only shortens the total time for internal oxidation by virtue of the reduced distance that oxygen has to diffuse, but also results in a more uniform microstructure. The present work was carried out with a view to quicken the process of oxidation further and to obtain a finer and more uniform dispersion. Rapidly solidified powder of composition Ag–6.0Sn–3.0In has been studied in view of its commercial importance as electrical contact material. Needless to say, rapid solidification leads to small grain size materials of more uniform composition [6]. A higher percentage of grain-boundary area is expected to facilitate faster diffusion of oxygen and hence to expedite the process of internal oxidation.

The role of indium in this alloy is to facilitate the internal oxidation of tin. It has been established that a tin content of more than 4 wt % is not amenable to internal oxidation because an impervious layer of tin oxide is formed, inhibiting further diffusion of oxygen [7]. Because indium forms a much stabler oxide than tin (free energy of formation of In_2O_3 at 298 K is $-830.93\ kJ\ mol^{-1}$ and that of SnO_2 $-519.77\ kJ\ mol^{-1}$), the uniformly distributed elemental indium becomes oxidized at a lower oxygen concentration than tin. The In_2O_3 particles become nuclei for the precipitation of tin oxide and may also enhance the rate of precipitation. These insoluble submicroscopic particles greatly increase the amount of high-energy interface region, thereby enhancing the diffusion of oxygen.

2. Experimental procedure

The flow chart of the adopted process route is given in Fig. 1. Alloy of composition Ag–6.0Sn–3.0In was prepared by vacuum resistance melting. The alloy melt was atomized in an atomizer consisting of an annular nozzle design of convergent–divergent geometry. The throat to exit ratio of the nozzle was designed to be 1:4. Atomization was carried out in a nitrogen atmosphere at 1.5 MPa pressure. The atomization conditions, such as nozzle position and optimum range of gas pressures, etc., were optimized using lead–tin alloy. The atomized powders were sieved through 150 mesh (ASTM) size sieve. The morphology of the powder was determined by scanning electron microscopy (SEM). The size distribution and microstructure of the atomized powder were determined by embedding them in Perspex™ thermoplastic.

In order to select the internal oxidation (IO) temperature, the melting point of the alloy composition was evaluated by differential scanning calorimetry

0022–2461

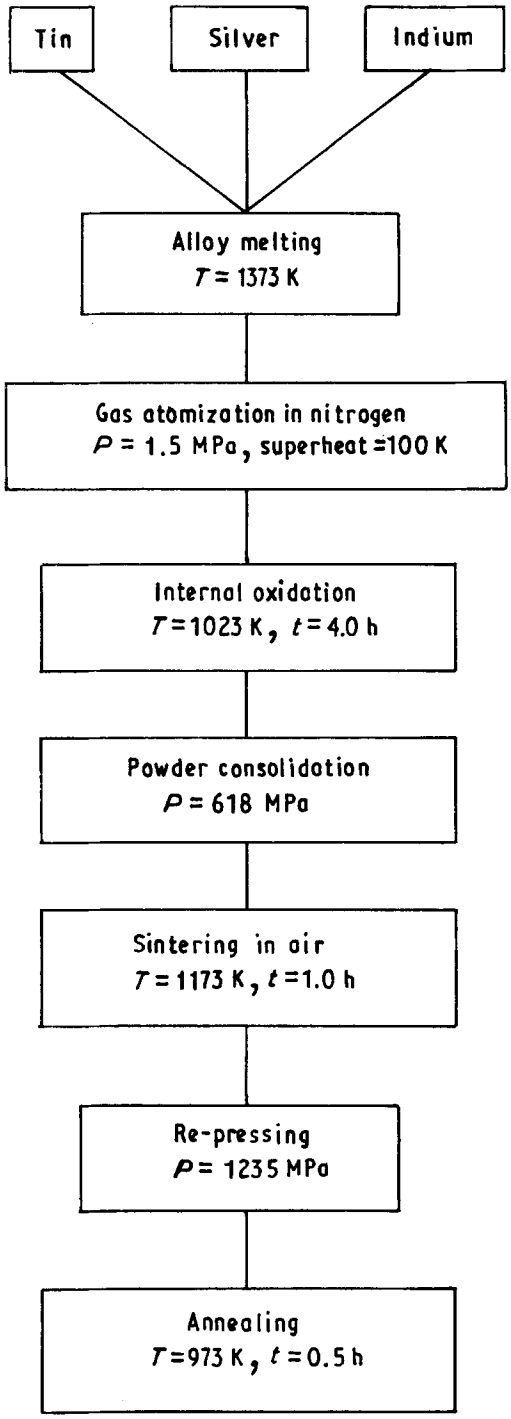

Figure 1 Flow diagram of the process.

(DSC). The internal oxidation behaviour of the representative sample was studied using a thermal gravimetric analyser (TGA). The powders were heated in air at the rate of 20 K min^{-1} to 1023 K followed by isothermal heating for 2 h at 1023 K. In order to compare the internal oxidation behaviour of the rapidly solidified atomized powders with the powders of coarser grain size, a small volume of powder was taken and heated in vacuum at 773 K for 24 h to bring about grain growth. The powder mass was well dispersed during this process to avoid sintering. The thermogram of these powders was determined in the same way as for the rapidly solidified atomized powders.

The morphology and microstructure of the as-atomized powder were determined. Having determined the time for internal oxidation by TGA, the complete mass of powder was internally oxidized at the same temperature, for durations longer than that determined by TGA, because of the denser packing of powders in the furnace. The internally oxidized powders were consolidated in the shape of cylindrical pellets of dimensions 16 mm diameter and 4 mm height. The consolidation was carried out in a double-acting hydraulic press at 618 MPa pressure. The green density of the pellets was determined by a dimensional method. The pellets were sintered in air at 1173 K for 1.0 h and density of the pellets was determined. The pellets were re-pressed at 1235 MPa pressure to improve the density. Re-pressed pellets were annealed at 973 K for 30 min. Electrical conductivity, hardness, density and microstructure of the annealed pellets were then evaluated. In order to determine the compositional variation from point to point, an X-ray line trace was taken using an energy dispersive spectrometer (EDS).

3. Results and discussion

It was earlier established [8] through X-ray studies that the combined percentage of tin and indium in Ag–6.0Sn–3.0In had terminal solubility in silver. The DSC scan of the alloy (Fig. 2) helped in determining the melting point of the alloy (1108.6 K) and thereby choosing a proper internal oxidation temperature.

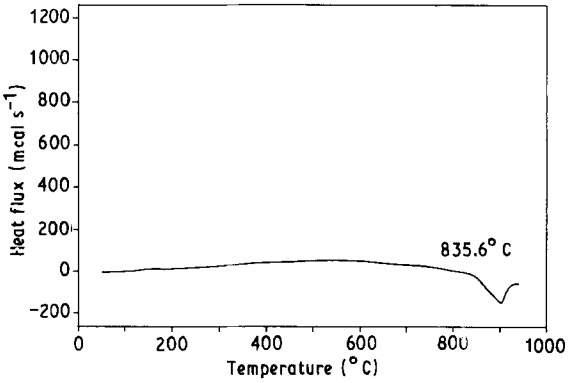

Figure 2 DSC scan of the Ag–6.0Sn–3.0In alloy.

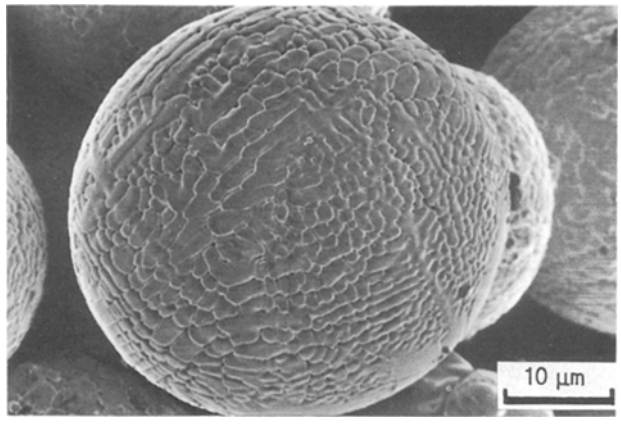

Figure 3 Scanning electron micrograph showing the morphology of rapidly solidified atomized powders.

The morphology of the as-atomized alloy powders, determined by SEM, is shown in Fig. 3. The surface features of the powders resemble powders processed by rapid solidification techniques. The spherical shape of the powders indicates the efficient disintegration of the melt stream by the rapidly expanding gas in the atomizer, and subsequent solidification before being collected. The particle-size distribution of the powder, as determined by image analysis, is shown in Fig. 4. It may be noted that about 70% powders are below the size of 70 μm. It is, therefore, expected that a high percentage of powders experienced high cooling rate during solidification. The microstructure of the powders (Fig. 5a) revealed fine dendrites, which confirmed the rapid solidification of the powders. In the absence of any established relation between the cooling rate and dendrite arm spacing for these alloys, the structure of these powders was compared with the microstructure of the master alloy (Fig. 5b). Considerable refinement of the dendrites is evident in the rapidly solidified powder, by comparison. Moreover, the appearance of second phase may also be noticed in the rapidly solidified powders, perhaps resulting from the non-equilibrium solidification of the composition.

TGA thermograms of the rapidly solidified powders and that of normal solidified powders, also referred to as coarse-grained material in the later text, are shown in Fig. 6. In order to compare the results, almost the same amount of the two types of powder were used for thermal analysis. It may be observed that in the beginning, kinetics of internal oxidation for the rapidly solidified powders is faster than that of the coarse-grained powders. Subsequently, both the powders seem to be oxidizing at the same rate. However, the rapidly solidified powders reach the saturation level, i.e. the completion of the reaction, earlier than the coarse-grained powders. The faster kinetics of rapidly solidified powders may be attributed to the

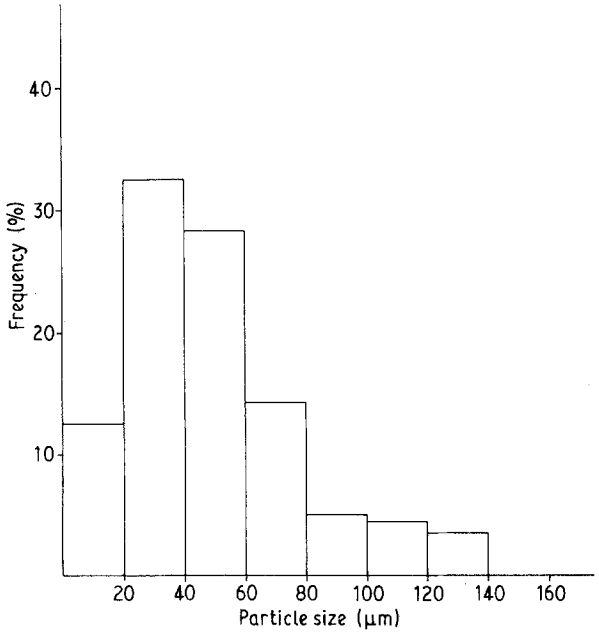

Figure 4 Particle-size distribution of the rapidly solidified atomized powders.

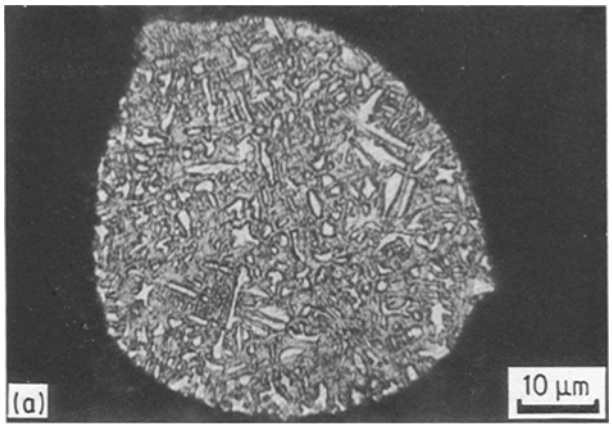

Figure 5 (a) Microstructure of the rapidly solidified atomized powder. (b) Microstructure of the master alloy.

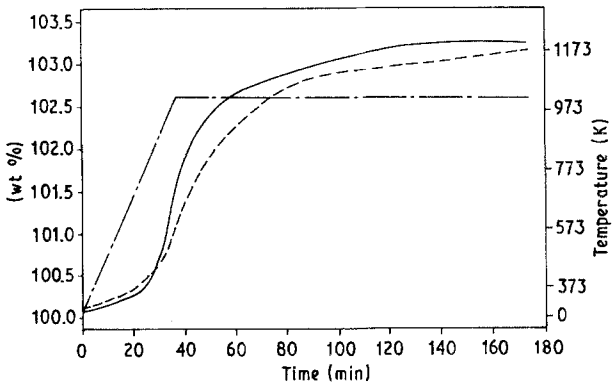

Figure 6 TG scan of the (——) rapidly solidified atomized powders, and coarse-grained powders subjected to (— — —) normal cooling and (— - —) the heating schedule.

enhanced grain-boundary diffusion of solute elements as well as oxygen. However, the kinetics of the reaction is retarded on prolonged heating due to grain coarsening simultaneous to precipitation of oxides of tin and indium along the grain boundaries. In order to plan the experiments, the time for internal oxidation was also estimated theoretically for the maximum diameter particle (i.e. 150 μm). For the purpose of approximate calculation the equations suggested earlier [3] for binary systems were used. This equation in its simplest form, involves the diffusion coefficient of oxygen, mole fraction of oxygen and solute, and stoichiometric constant of oxides. The diffusion coefficient and mole fraction of oxygen were calculated at 1023 K

using predetermined relations [9]. The combined mole fraction of tin and indium was used as solute mole fraction. The calculation showed that 150 μm powder of the composition would require less than 25 min for complete internal oxidation. However, the experimental values were found to be much higher. This shows that the equations valid for the internal oxidation of binary systems no longer hold good for ternary systems.

The morphology of the powders after internal oxidation is shown in Fig. 7. It is evident from the photograph that to a large extent the shape of the powders remains unchanged, but a number of blister-like features may be seen on the surface. The composition of these blisters was analysed with the help of EDS. EDS analysis showed the blisters to be composed of mainly silver with peaks of no other elements within the sensitivity of EDS. Formation of these blisters has been explained on the basis of a diffusional creep mechanism [10]. The microstructure of internally oxidized powders (Fig. 8) further corroborates the presence of silver-rich regions on the surface. Grain boundaries, marked by heavy oxide precipitation near the surface, may also be noted in the micrograph. This indicates that to begin with the oxidation is controlled by grain-boundary duffusion. Subsequently, the grain-boundary precipitation of oxides impairs the diffusion and retards the kinetics. Fine oxides of tin and indium can also be observed within the grains. However, due to their fineness, the oxide particles are not resolved in the optical micrographs. It has been established earlier by X-ray phase analysis that tin and indium exist as SnO_2 and In_2O_3 after internal oxidation [11].

Internally oxidized powders were consolidated to achieve a green density of 97.9% theoretical density. Upon sintering, insignificant change in dimensions as well as density was observed. The low shrinkage after sintering was attributed to the prevention of dislocation movement due to the fine dispersion of oxide particles in the silver matrix. Needless to say, dislocation movement has been identified as an important sintering mechanism in the early stages of densification of silver [12]. After re-pressing and annealing, a final density of 98.2% theoretical was obtained.

The microstructure of the sintered compacts was observed at low and high magnifications as shown in Fig. 9a and b, respectively. The low-magnification micrograph reveals the overall microstructure of the sample. It may be noted that each particle is separated from the adjoining particle by a thin layer, devoid of oxides. An EDS trace of silver was taken along the line and the corresponding map is shown in the micrograph. Higher X-ray counts were recorded at the boundaries and in the middle of bigger particles. The phenomenon responsible for the higher percentage of

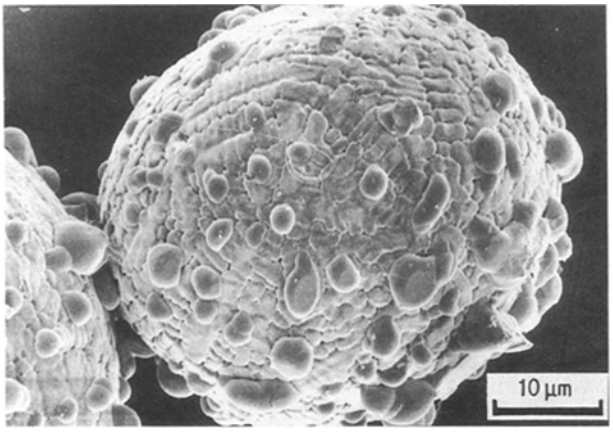

Figure 7 Morphology of the rapidly solidified atomized powders after internal oxidation.

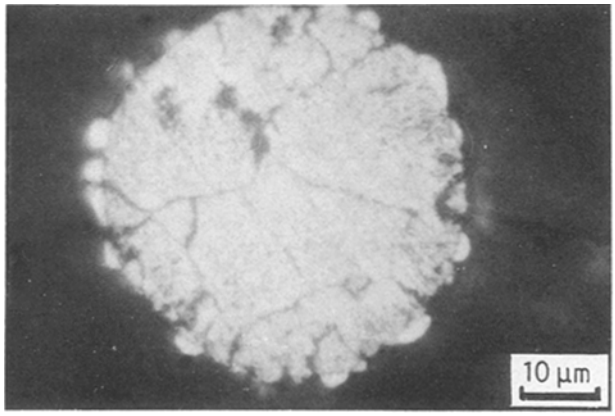

Figure 8 Microstructure of the rapidly solidified powders after internal oxidation.

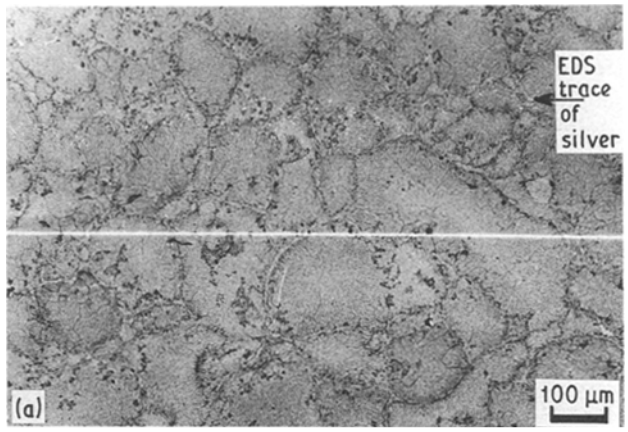

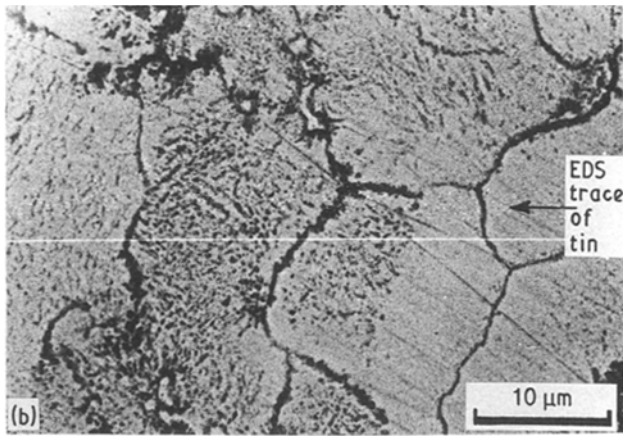

Figure 9 (a) Scanning electron micrograph along with EDS trace (silver) of the compacts prepared from internal oxidation of rapidly solidified powders. (b) Scanning electron micrograph along with EDS trace (tin) of the compacts prepared from internal oxidation of rapidly solidified powders.

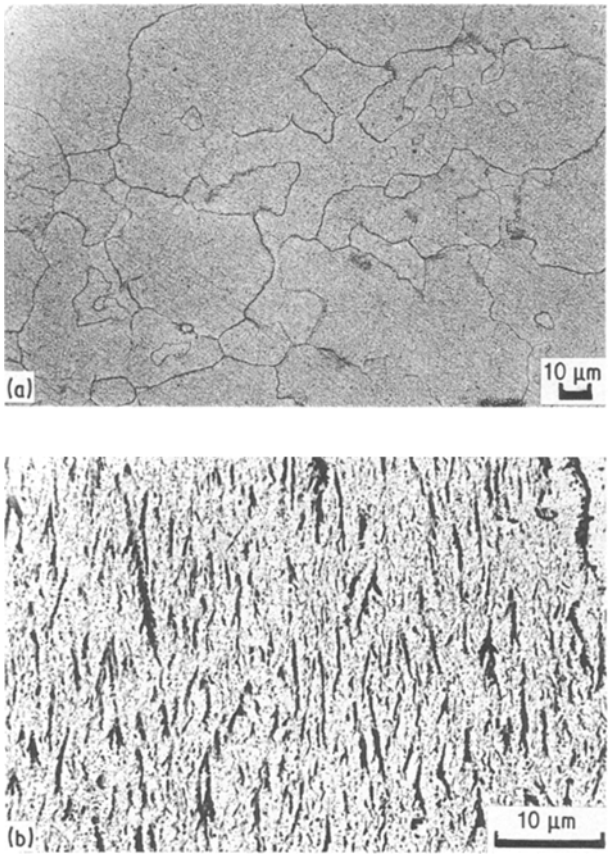

Figure 10 (a) Scanning electron micrograph of the internally oxidized Ag–6.0Sn–3.0In alloy; section transverse to diffusing oxygen front. (b) Scanning electron micrograph of the internally oxidized Ag–6.0Sn–3.0In alloy; section longitudinal to diffusing oxygen front.

silver on the surface of particles has been explained earlier. However, the higher X-ray counts in the centre of larger particles is due to the formation of denuded zones in these particles. While a high degree of solute redistribution does not occur in the smaller particles, the effect is more pronounced in the bigger particles. The high-magnification micrograph (Fig. 9b) revealed heavy precipitation of oxides along the grain boundaries and virtually oxide-free regions in the vicinity. This phenomenon is described as a divorced grain boundary [13] and is attributed to the increased diffusion of oxygen along the grain boundaries. An EDS trace for tin was taken along the line shown in Fig. 9b. The low X-ray counts in the depleted region further support the microscopy results. The shape of the oxide particles seems to be equi-axed with a tendency to grow in the direction of advancing diffusion front.

The relevant physical properties of the compacts such as electrical conductivity, hardness and density were compared with the materials prepared by conventional internal oxidation of alloy pellets [8]. These properties are compared in Table I, whereas the microstructure of the internally oxidized pellet is given in Fig. 10a and b. The physical properties of the compacts prepared by rapidly solidified alloy powders compare well with the internally oxidized alloy pellets. As far as the microstructure is concerned, the low-magnification micrograph (Fig. 10a), taken on the transverse section to the diffusion of oxygen, shows bigger grains than that obtained by the internal oxidation of rapidly solidified alloy powders. The microstructure in the longitudinal section (Fig. 10b) of the internally oxidized pellet reveals needle-shaped oxide particles extending along the direction of diffusing oxygen front. However, due to the small particle size and isotropic diffusion of oxygen, no such effect was observed in the samples prepared by using internally oxidized powders. Needless to say, a fine dispersion of oxides is one of the most sought after microstructural characteristics in these materials from the point of view of performance.

4. Conclusions

The present study sheds light on the internal oxidation behaviour of rapidly solidified alloy powders. It helps us to understand the influence of process on the relevant physical properties of an alloy composition, which has gained commercial importance in the recent years. The following points can be concluded from the study.

1. It has been shown that in the initial stages of internal oxidation of rapidly solidified alloy powders, the kinetics is faster than for the coarse-grained powders. However, only a marginal gain, in terms of time, ultimately results due to precipitation of oxides along the grain boundary.

2. The theoretical results of kinetics given by previous workers for internal oxidation of binary alloys cannot be used for ternary systems like Ag–Sn–In. In the ternary system, the kinetics does not seem to depend solely on the diffusion coefficient of species and their mole fraction, but the morphology and microstructural development with the progress of oxidation also have a significant effect.

3. The theoretical treatments of the internal oxidation process, as perceived by the earlier workers, do not take into account the influence of grain size on the

TABLE I Important physical properties of internally oxidized Ag–6.0Sn–3.0In materials

Process	Electrical conductivity (% IACS)[a]	Average hardness ($HV_{0.5}$)	Density ($g\ cm^{-3}$)	Theoretical density (%)
Internal oxidation of rapidly solidified alloyed powders	65.0	109.0	9.81	98.2
Internal oxidation [8]	65.0	108.2[b]	9.99	100

[a] 100% IACS = 58 $m\Omega^{-1}\ mm^{-2}$ or Siemens.
[b] Measured at the depth of 0.05 mm from surface.

overall kinetics of internal oxidation process. However, it has been brought out in the present study that grain size does play a role in the kinetics and development of microstructure of the internally oxidized materials.

4. The microstructure of the samples prepared by internal oxidation of rapidly solidified powders has a fine dispersion of oxides. However, there is a large volume of material, in the vicinity of grain boundaries, depleted of oxides. This is not favourable as far as the anti-erosion and anti-welding properties of these materials in the end use is concerned.

Acknowledgement

The authors thank Mr B. N. Banerjee for fabricating the atomizer. The experimental assistance of Mr Piush Verma and Mr Sarbjit Singh is gratefully acknowledged.

References

1. C. WAGNER, *Z. Electrochem.* **63** (1959) 772.
2. R. A. RAPP, *Acta Metall.* **9** (1961) 730.
3. F. N. RHINES, *Trans. Amer. Inst. Min. (Metall.) Eng.* **137** (1940) 246.
4. F. N. RHINES, W. A. JOHNSON and W. A. ANDERSON, *Trans. Met. Soc. AIME* **147** (1942) 205.
5. D. J. PEDDER, P. DOUGLASS, J. P. MacCARTHY and F. S. BUGNES, *IEEE Trans.* **PHP13** (1977) 42.
6. T. R. ANANTHARAMAN and C. SURYANARAYANA, "Rapidly Solidified Metals – A Technological overview" (Trans. Tech, Aedermannsdorf, Switzerland, 1987).
7. Y. S. SHEN and L. J. GOULD, *IEEE Trans.* **CHMT-4** (1987) 157.
8. A. VERMA and T. R. ANANTHARAMAN, *Bull. Mater. Sci.* **14** (1991) 1.
9. W. EICHENAUER and G. MULLER, *Z. Metallkde* **53** (1962) 321.
10. J. RODWAY MACKERT Jr., *Metall. Trans.* **17A** (1986) 746.
11. A. VERMA, A. ROY and T. R. ANANTHARAMAN, *Int. J. Powder Metall.* **27(1)** (1991) 51.
12. J. E. SHEEMAN, F. V. LENEL and G. S. ANSELL, *Mater. Sci. Res.* **C** (1972) 201.
13. Y. S. SHEN, E. J. ZDANUK and R. H. KROCK, in "Proceedings of the Sixth International Conference on Electrical Contact Phenomena", Chicago (1972) p. 333.

Received 17 July
and accepted 27 November 1991